DOI 10.1007/s10891-019-01942-6

Journal of Engineering Physics and Thermophysics, Vol. 92, No. 2, March, 2019

MODELING THE SYNTHESIS OF COMPOSITE TITANIA- AND SILICA-BASED CORE–SHELL TYPE PARTICLES IN A PLASMACHEMICAL REACTOR

S. M. Aul′chenko[a,b] and E. V. Kartaev[a]

UDC 532.075.8

One-stage synthesis of composite titania and silica nanoparticles in the working area of a plasmachemical reactor by a chloride method, which is based on separate oxidation of titanium and silicon tetrachlorides, has been modeled for the first time. The influence of a number of parameters of the physicomathematical model on both the general size of the particles and the shell thickness has been investigated. Results of calculations for certain variants of the parameters have been given.

Keywords: *titania, silica, composite particle, plasmachemical reactor, one-velocity multicomponent medium, homogeneous and heterogeneous reactions, coagulation.*

Introduction. One of the most promising trends in today′s technologies is the synthesis of nanocomposite powders of oxide ceramics belonging to a new class of materials with physicochemical properties controllable over a wide range depending on their purpose. In particular, wide use has been enjoyed by nanosize titania (TiO_2) particles. Here, in many applications of practical importance, it is required that photocatalytic activity of TiO_2 particles be suppressed, e.g., in pigmentary titania additives to dyes and plastic and in the production of paper and sunscreens. In this case it is required that the area of the photoactive free surface of titania be as small as possible, with the optical properties of the material itself being preserved. This requirement is met by, e.g., nanocomposite titania and silica (TiO_2 + SiO_2) particles of the "core–shell" structure. Here, the larger the thickness of the amorphous SiO_2 layer and the smaller its microporosity, the stronger is the reduction in the photoactivity of composite nanopowder [1].

In the present work, from the program created by the authors to calculate flows of a multicomponent reactive gas mixture, which is based on the algorithms of solution of a quasi-gasdynamic system of equations, the synthesis of nanocomposite TiO_2 + SiO_2 particles of this structure in a flow-type plasmachemical reactor was modeled for the first time. In modeling, the authors implemented a one-stage method of production of the sought powders. In the channel′s upper part, titanium tetrachloride $TiCl_4$ in a vapor phase is fed to the reactor. In the reactor zone ahead of the unit of feeding tetrachlorosilane $SiCl_4$, there occurs conversion of titanium tetrachloride with formation of TiO_2 particles with their subsequent growth due to the surface reaction and coagulation. Studies [2–4] give results of calculations and experiments of this stage. In the region of mixing $SiCl_4$ with the mainstream the gas phase of silica SiO_2 is formed. At a small ratio of the concentrations of the $SiCl_4$/$TiCl_4$ vapors, the silica vapor condenses just on the surface of titania particles to form a shell without forming individual SiO_2 particles [5]. Furthermore, the shell thickness may also grow due to the surface reaction. The gas in the plasma-generating jet is nitrogen with a temperature of 4500 K. A scheme of premixing of the reactants (titanium tetrachloride and tetrachlorosilane with an air oxygen) outside the reactor is used.

Difficulties with modeling physicochemical processes in flows of chemically active gases are associated with the absence of reliable data on transfer coefficients in high-velocity gas flows, on rigorous temperature boundaries of reactions and phase transitions, etc. All this assumes a considerable volume of parametric calculations to verify modeling results. In the present work, for the reactor whose shape and dimensions correspond to an actual laboratory setup, the calculations have been carried out for a number of values of the constants of a physicomathematical model and of operating regimes.

Formulation of the Problem. Figure 1 shows a diagram of the working area of a flow-type reactor (the actual position is vertical). A nitrogen jet with temperature T_1 and with flow rate Q_1 flows into the working area through a channel.

[a]S. A. Khristianovich Institute of Theoretical and Applied Mechanics, Siberian Branch of the Russian Academy of Sciences, 4/1 Institutskaya Str., Novosibirsk, 630090, Russia; [b]Novosibirsk State University of Architecture and Civil Engineering, 159 Turgenev Str., Novosibirsk, 630008, Russia; email: aultch@itam.nsc.ru. Translated from Inzhenerno-Fizicheskii Zhurnal, Vol. 92, No. 2, pp. 397–403, March–April, 2019. Original article submitted February 27, 2017.

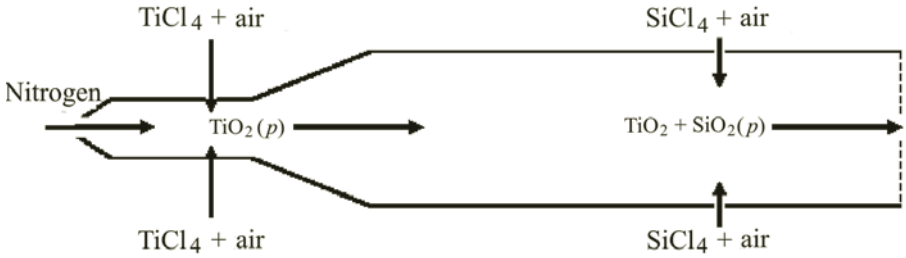

Fig. 1. Diagram of the working area of the flow-type reactor.

A mixture of titanium tetrachloride and air at the temperature T_2 with flow rate Q_2 is fed through the first lateral slot. In the mixing zone, a reaction proceeds to form first the gas-phase component of TiO_2, and then TiO_2 particles. Next, as the particles move along the reactor, they grow due to the surface reaction and coagulation. A mixture of silicon tetrachloride and air at the temperature T_3 with flow rate Q_3 is fed through the second lateral slot.

In the mixing zone, we have a homogeneous reaction to form the gas-phase component of SiO_2 which condenses on titania particles and a heterogeneous reaction to form a solid phase on the surface of both TiO_2 particles and composite $TiO_2 + SiO_2$ particles. It is assumed that there is no coagulation of the composite particles. This assumption will be checked experimentally.

Mathematical Model. We consider flow of a viscous heat-conducting mixture of gases. The components of the mixture are O_2, N_2, $TiCl_4$, $SiCl_4$, TiO_2, SiO_2, and Cl_2. The last three components result from the generalized chemical reactions

$$TiCl_4 + O_2 \xrightarrow{k_T} TiO_2 + 2Cl_2 , \quad SiCl_4 + O_2 \xrightarrow{k_S} SiO_2 + 2Cl_2 .$$

Consideration is given to a one-fluid regime of flow which is modeled using the system of quasi-gasdynamic equations [2]. With account for external forces and heat sources, this system is of the form

$$\frac{\partial \rho}{\partial t} + \operatorname{div} \mathbf{j} = 0 ,$$

$$\frac{\partial (\rho \mathbf{u})}{\partial t} + \operatorname{div} (\mathbf{j} \otimes \mathbf{u}) + \nabla p = \rho \mathbf{F} + \operatorname{div} \Pi , \tag{1}$$

$$\frac{\partial (E)}{\partial t} + \operatorname{div} (\mathbf{j} H) + \operatorname{div} \mathbf{q} = (\mathbf{j}\mathbf{F}) + \operatorname{div} (\Pi \mathbf{u}) + Q .$$

The vector of the mass-flux density is determined by the following relation:

$$\mathbf{j} = \rho \mathbf{u} - \tau [\operatorname{div} (\rho \mathbf{u} \otimes \mathbf{u}) + \nabla p - \rho \mathbf{F}] , \quad \tau = \frac{M}{\operatorname{Re} \operatorname{Sc}} \frac{T}{p} .$$

This system is supplemented with the continuity equations for the mixture′s components:

$$\frac{\partial \rho_i}{\partial t} + \operatorname{div} \mathbf{j}^i = \sum_j J^{(ji)} \tag{2}$$

and the volume concentration of the solid phase

$$\frac{\partial c_p}{\partial t} + \operatorname{div} (c_p \mathbf{u}) = \sum_j J^{(jp)} . \tag{3}$$

On the right-hand sides of Eqs. (2) and (3), account has been taken of the following relations describing the change in the concentrations of titanium tetrachloride and titania in the gas and solid phases, and also of silicon tetrachloride and silica in the gas and solid phases due to the homogeneous and heterogeneous reactions and to the phase transition:

$$\frac{dC^1}{dt} = -k_T^r C^1 = -\left(k_T^h + k_T^s A\right) C^1 , \quad \frac{dC^2}{dt} = k_T^h C^1 - k_T^{ph} C^2 ,$$

$$\frac{dC^3}{dt} = k_T^s C^1 A + k_T^{ph} C^2 , \quad \frac{dC^4}{dt} = -k_S^r C^4 = -\left(k_S^h + k_S^s A\right) C^4, \tag{4}$$

$$\frac{dC^5}{dt} = k_S^h C^4 - k_S^{ph} C^5 , \quad \frac{dC^6}{dt} = k_S^s C^4 A + k_S^{ph} C^5 .$$

Additional relations closing the system of equations are of the form

$$p = \rho R_m T \frac{m_g}{1 - c_p} , \quad \alpha_i = \rho_i / \rho , \quad R_m = R_g \left(\sum_i \alpha_i / m_i \right) .$$

If relations (1)–(4) are supplemented with the equation for the number of particles:

$$\frac{dN}{dt} = k_T^h C^1 N_{Av} - \frac{\beta N^2}{2} , \tag{5}$$

then with account for their known initial diameter d_0 and knowing the mass of the particles and their number and volume concentration in each computational cell at each instant of time, we can calculate the size of particles.

The coagulation parameter, according to [6], has been calculated from the formula

$$\beta = 8\pi d_B d_p \left[\frac{d_p}{d_p + g\sqrt{2}} + \frac{4 d_B \sqrt{2}}{u_p d_p} \right]^{-1} ,$$

where $g = \left(\frac{1}{3 d_p l_a} \right) \left[(d_p + l_a)^3 - (d_p + l_a)^{\frac{3}{2}} \right] - d_p$, $l_a = \frac{8 d_B}{\pi u_p}$, and $d_B = \frac{3\sqrt{mkT/2\pi}}{2\rho d_p^2 (1 + \alpha\pi/8)}$.

Boundary Conditions. On the reactor walls, we adopted the adhesion conditions, the absence of the heat flux, and the equality of the normal pressure derivative to zero (this additional condition is caused by the special features of the system of quasi-gasdynamic equations). For the jets, we assign the flow rate and temperature. To calculate the values of pressure, density, and velocity at the inflow boundaries of the jets, we use boundary conditions which are based on the Riemann invariants for Euler equations.

In numerically integrating Eqs. (1)–(3), they are written in a cylindrical coordinate system (the problem is axisymmetric) and are reduced to a dimensionless form. As the problem′s basic dimensional parameters we select the channel radius and the velocity of sound in quiescent air at a temperature of 300 K in the reactor at the initial instant of time and the air density.

For numerical solution of the system of equations, we use a time-explicit difference scheme. Time derivatives are approximated by forward differences with the first order of accuracy. Space derivatives are approximated by central differences with the second order of accuracy.

Calculation Results. The main series of calculations whose results can be verified with experimental data was conducted in the following statement. At the first stage, we calculated a quasi-stationary flow field in the reactor, which was formed by injecting the jet from a plasmatron. Thereafter, lateral jets were injected.

The geometric characteristics of the reactor were $L_R = 444$ mm, $d_R = 32$ mm, $L_C = 38$ mm, $d_C = 7$ mm, $L_{Tr} = 33$ mm, and $\alpha^0 = 15^o$. The coordinates of the midlines of slots for injection of lateral jets were $z_1 = 28$ mm and $z_2 = 292$ mm.

The parameters in the setup were $T_1 = 4500$ K, $Q_1 = 1$ g/s, $T_2 = 490$ K, $Q_2 = 2.5$ g/s, $T_3 = 490$ K, and $Q_3 = 2.2$ g/s. The composition of the first lateral jet was as follows: 80% air and 20% $TiCl_4$; the composition of the second lateral jet was 96.7% air and 3.3% $SiCl_4$.

According to [6, 7], the assigned basic values of the constants in Eqs. (4) and (5) were as follows:

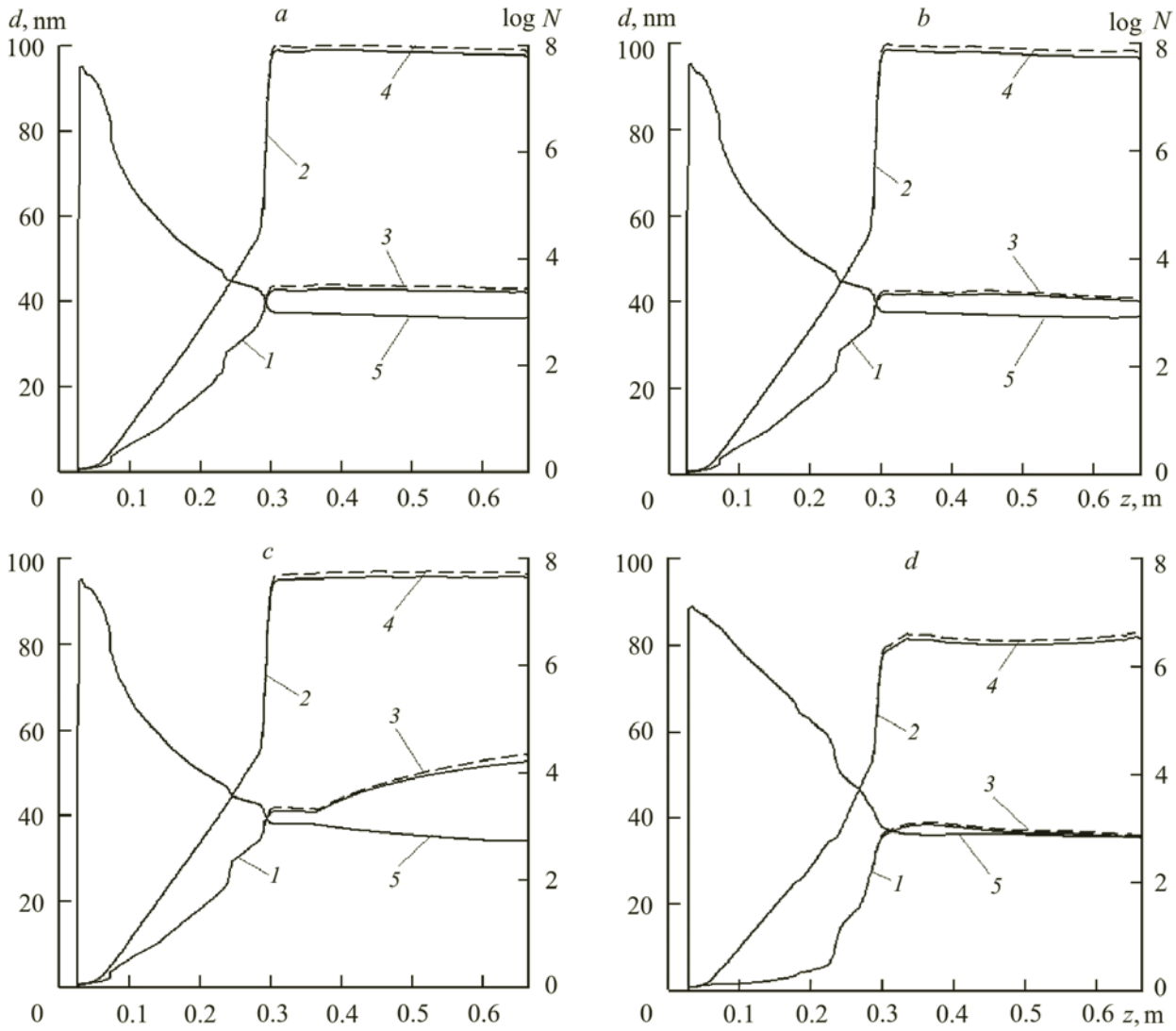

Fig. 2. Lengthwise distribution of the weighted mean diameter of particles and of the logarithm of the number of particles in the reactor: a) calculation with the model′s basic parameters, b) calculation with $k_S^s = 0$, c) calculation with $k_S^{ph} = 0$, and d) calculation with the model′s basic parameters with a higher than average share of $SiCl_4$; 1) diameter of TiO_2 particles averaged over the number of the particles, 2) diameter of TiO_2 particles averaged over their mass, 3) diameter of composite particles averaged over the number of the particles, 4) diameter of composite particles averaged over their mass, and 5) logarithm of the number of particles.

$$k_T^r = 8.26 \cdot 10^4 \exp\left(\frac{-10{,}681}{T}\right), \quad k_T^s = 4.9 \cdot 10^3 \exp\left(\frac{-8993}{T}\right), \quad k_T^{ph} = 1.2 \cdot 10^{10} \exp\left(\frac{-10{,}681}{T}\right),$$
$$k_S^r = 8.0 \cdot 10^{14} \exp\left(\frac{-400{,}000}{T}\right), \quad k_S^s = 4.0 \cdot 10^{13} \exp\left(\frac{-40{,}828}{T}\right), \quad k_S^{ph} = k_T^{ph}. \tag{6}$$

In the available literature, the values of constants for $SiCl_4$ conversion differ by an order of magnitude, and there is no information on the nucleation rate. These parameters need to be refined on the basis of experimental data.

Figure 2 gives the distributions along the reactor of the weighted mean diameters of particles by their number $d_i = \frac{1}{N_i}\sum_j d_{ij}N_{ij}, N_i = \sum_j N_{ij}$ and mass $d_i = \frac{1}{M_i}\sum_j d_{ij}m_{ij}$, $M_i = \sum_j m_{ij}$, and also the distribution of the values of the logarithm of the number of particles for different values of the model′s parameters and operating regimes of the reactor. Figure 2a gives the calculation results corresponding to the model with basic parameters (6). Figure 2b and c gives the results of calculations from the model in which $k_S^s = 0$ and $k_S^{ph} = 0$, respectively.

These calculations were done so as to assess the contribution of the surface reaction of oxidation of silicon tetrachloride and of gas-phase condensation of silica to the growth in the silica shell. Figure 2d gives the results of calculation from the model with basic parameters, but with a thrice as high content of silicon tetrachloride in the second lateral jet. Common to all the regimes is a monotonic growth in the dimensions of titania particles on the portion between the zones of injection of the first and second lateral jets followed by a stepwise growth in the region of injection of the second jet. This growth occurs in the process of coagulation of the particles with the resulting decrease in their number by the law of (5), whereas the jump is due to the contraction of the flow core by the lateral jet leading to a sharp growth in the value of the second term in expression (5). The difference in particle dimensions obtained by averaging over the particles' number and mass is due to a certain nonuniformity in the particle size distribution in the reactor cross sections. The major part of particles is concentrated in the flow core, whereas the minor part, but of larger particles, is near the walls. This is due to the smaller velocity of the flow near the walls, accordingly, with increase in the time during which we have a growth in TiO_2 particles due to the surface reaction and coagulation. In the regimes presented in Fig. 2a,b, and d, coagulation of particles does not occur downstream of the region of mixing of the mainstream with the second lateral jet, since practically a SiO_2 shell has already been formed on all the TiO_2 particles and the absence of coagulation between the composite particles has been included in the model. The influence of the model′s parameters on the size and structure of composite particles is more than direct as a rule. For example, on the values of the rate constants of the surface reaction and condensation k_S^s and k_S^{ph}, there depends not only the rate of buildup of the shell on the particle but also the position of the boundary of passage of TiO_2 particles into composite particles and hence the cessation of their growth due to coagulation. The region of propagation of the gas phase of TiO_2 and hence of its possible condensation on the particle′s surface is much larger than the region in which we can have a surface reaction. This explains the proximity of the curves in Fig. 2a and b. The number of the particles is identical, in practice. The dimensions of the core (average over the number of particles) of a composite particle are 42.5 and 40.3 nm respectively. The smaller dimension of the core at $k_S^s = 0$ is attributed by the upstream shift of the boundary of formation of composite particles due to the increase in the share of the TiO_2 gas phase. For the regimes presented in Fig. 2a and b, the dimensions of the composite particles (average over the number of particles) at exit from the reactor are 43.3 and 40.9 nm. In the first variant, the shell thickness is 0.2 nm greater. This difference is attributed to both the contribution of the surface reaction and the difference, even if small, in the number of particles. Since in the second variant their number is larger, the shell thickness is smaller at the same mass. The results presented in Fig. 2c show how great the role of the position of the boundary of transition of TiO_2 particles to $TiO_2 + SiO_2$ particles is. The displacement of this position downstream at $k_S^{ph} = 0$ leads to a growth in the dimensions of the core to 52.3 nm and, accordingly, to a larger thickness of the shell, i.e., 1.6 nm, on averaging over the number of particles. Decrease in the average dimensions of mass-averaged TiO_2 particles in the third variant (Fig. 2c) down to 95.7 nm from 98.0 nm and 97.1 nm in the first and second variants, respectively, is due to the fact that the region of the surface reaction is closer to the reactor wall and it is the largest particles that are first to find themselves in it. Naturally, when the shell is formed by just one reaction its total mass is smaller as indicated by mass-average dimensions of composite particles of 99.3, 98.1, and 96.9 nm in variants a, b, and c, respectively. Figure 2d gives the results of calculation of the synthesis of composite nanoparticles for the variant of the setup′s operating regime with an $SiCl_4$ share in the second lateral jet thrice (10%) as great and basic values of the model′s parameters. The shell has begun to form predictably earlier and hence the dimension of the particle′s core is much smaller (and the number of particles is nearly twice as large): in the number-average particles, 35.6 nm, and in the mass-average ones, 81.7 nm. Shell thicknesses of 0.5 and 1.0 nm at final dimensions of 36.1 and 82.7 nm point to the increase in the share of SiO_2 in a composite particle with increase in the supplied $SiCl_4$ mass.

Conclusions. One-stage synthesis of composite titania and silica nanoparticles in the plasmachemical-reactor′s working area by a chloride method which is based on separate oxidation of titanium and silicon tetrachlorides has been modeled for the first time. The influence of a number of parameters of the physicomathematical model and of regime parameters of the setup on both the general size of the particles and the shell thickness has been investigated. Results of calculations for certain variants of the parameters have been given. These results, and also those that will be obtained in subsequent parametric

investigations combined with the data of experiments to be conducted on the created laboratory setup will make it possible to refine the parameters of the model and to control the characteristics of the produced composite particles.

Acknowledgment. This work was carried out with partial financial support from the Russian Foundation for Basic Research (grant No. 18-08-00219a).

NOTATION

A, relative area of particles, cm^2/cm^3; C^1, C^2, C^3, C^4, C^5, and C^6, concentrations of titanium tetrachloride and titania in the gas phase and of titania in the solid phase, of silicon tetrachloride and silica in the gas phase, and of silica in the solid phase, mole/cm^3; c_p, volume concentration of the solid phase; Cl_2, chlorine; d_B, diffusion coefficient of a Brownian particle, m^2/s; d_C and d_R, channel and reactor diameters, mm; d_p, diameter of particles, nm; d_0, initial diameter of particles, nm; d_i, weighted mean diameter of a particle in the ith cross section, nm; d_{ij}, diameter of a particle in the jth computational cell of the ith cross section, nm; E, normalized total energy of a unit volume; $\mathbf{F}$, normalized vector of the mass-force density; H, normalized total specific enthalpy; $J^{(ji)}$, normalized intensity of transformation of the mass of the jth component into the ith component in a unit volume of the mixture; $J^{(jp)}$, normalized intensity of transformation of the mass of the jth component into a solid phase in a unit volume of the mixture; $\mathbf{j}$, normalized vector of the mass-flux density of the mixture; $\mathbf{j}^i$, normalized vector of the mass-flux density of the ith component; k_T^r and k_S^r, rates of generalized reactions, 1/s; k, Boltzmann constant, J/K; k_T^h and k_S^h, rates of homogeneous reactions, 1/s; k_T^s and k_S^s, rates of surface reactions, cm/s; k_T^{ph} and k_S^{ph}, rates of phase transitions, cm^3/s; L_C, L_R, and L_{Tr}, lengths of the channel, the reactor, and the transition tube, mm; M, Mach number; m, mass of a carrier-gas molecule; m_g, mass fraction of the gas; M_i, particles' mass in the ith cross section; m_i, molecular weight of the ith component; m_{ij}, particles' mass in the jth computational cell of the ith cross section; N, number of particles in a unit volume; N_{Av}, Avogadro number; N_i, number of particles in the ith cross section; N_{ij}, number of particles in the jth computational cell of the ith cross section; N_2, nitrogen; O_2, oxygen; p, normalized pressure; Q, normalized heat; Q_1, rate of flow of the nitrogen jet from the plasmatron, g/s; Q_2 and Q_3, rates of flow of the first and second lateral jets, g/s; Re, Reynolds number; R_g, specific gas constant, J/(kg·K); R_m, specific gas constant of the mixture, J/(kg·K); $SiCl_4$, silicon tetrachloride; SiO_2, silica; Sc, Schmidt number; t, time, s; T, normalized temperature; T_1, temperature of the nitrogen jet from the plasmatron, K; T_2 and T_3, temperatures of lateral jets, K; $TiCl_4$, titanium tetrachloride; TiO_2, titania; $\mathbf{u}$, normalized velocity vector of the mixture; u_p, velocity of particles, m/s; z, axis of the cylindrical coordinate system; z_1 and z_2, coordinates of the midlines of the slots for injection of lateral jets; α, accommodation coefficient; α^0, slope of the transition tube, deg; α_i, mass fraction of the ith component; β, coagulation parameter, cm^3/s; Π, normalized viscous-stress tensor; ρ, normalized density of the mixture; ρ_i, normalized density of the ith component; τ, normalized relaxation parameter. Subscripts and superscripts: C, channel; h, homogeneous; m, mixture; p, particle; s, surface; S, silicon; T, titanium; Tr, transition; R, reactor; r, reaction

REFERENCES

1. A. M. El-Toni, S. Yin, and T. Sato, Control of silica shell thickness and microporosity of titania–silica core–shell type nanoparticles to depress the photocatalytic activity of titania, *J. Colloid Interface Sci*., **300**, No. 1, 123–130 (2006).
2. S. M. Aul′chenko, Controlling the process of titanium dioxide nanoparticle growth in a continuous-flow plasma-chemical reactor, *J. Eng. Phys. Thermophys*., **86**, No. 5, 1027–1034 (2013).
3. E. V. Kartaev, V. P. Lukashov, S. P. Vashenko, S. M. Aulchenko, O. B. Kovalev, and D. V. Sergachev, Experimental study of the synthesis of the ultrafine titania powder in plasmachemical flow-type reactor, *Int. J. Chem. React. Eng*., **12**, No. 1 (2014); DOI: 10.1515/ijcre-2014-0001.
4. S. M. Aul′chenko and E. V. Kartaev, Control of the synthesis of submicron titanium dioxide particles in a continuous plasma-chemical reactor, *J. Eng. Phys. Thermophys*., **88**, No. 6, 1459–1465 (2015).
5. B. Buesser and S. E. Pratsinis, Design of gas-phase synthesis of core–shell particles by computational fluid–aerosol dynamics, *AIChE J*., **57**, No. 11, 3132–3142 (2011); DOI:10.1002/aic.12512.
6. A. Kolesnikov and J. Kekana, Nanopowders production in the plasmachemical reactor: modelling and simulation, *Int. J. Chem. React. Eng*., **9**, Article A83 (2011).
7. H. K. Park and K. Y. Park, Control of particle morphology and size in vapor-phase synthesis of titania, silica and alumina nanoparticles, *KONA Powder Particle J*., No. 32, 85–101 (2015).